UNIVERSITY OF PARDUBICE

FACULTY OF CHEMICAL TECHNOLOGY

Institute of Organic Chemistry and Technology

Ing. Zuzana Hloušková

Organic push-pull molecules serving photoredox catalysis

Theses of the Doctoral Dissertation

Pardubice 2019

Study program: **Organic Chemistry**

Study field: **Organic Chemistry**

Author: **Ing. Zuzana Hloušková**

Supervisor: **prof. Ing. Filip Bureš, Ph.D.**

Year of the defence: 2019

References

HLOUŠKOVÁ, Zuzana, *Organic push-pull molecules serving photoredox catalysis*, Pardubice, 2019. 123 Pages. Dissertation thesis (Ph.D.). University of Pardubice, Faculty of Chemical Technology, Institute of Organic Chemistry and Technology. Supervisor prof. Inf. Filip Bureš, Ph.D.

Abstract

A literature search focusing on visible light photoredox catalysis that utilizes organic substances has been accomplished. Overall, six classes of organic substances currently used as photoredox catalysts have been found and their phophysical and electrochemical properties and use in photoredox reactions has been summarized. The experimental part focuses on optimizing synthesis of the known photocatalyst. Subsequently, structural modifications of the original catalyst have been carried out leading to seventeen catalysts with acceptor part based on pyrazine-2,3-dicarbonitrile, pyrazine-3,5-dicarbonitrile, pyridine-2,6-dicarbonitrile, pyridine-4-carbonitrilu and pyridine-3,5-dicarbonitrile. Various peripheral donors such as thiophene, 2-methoxythiophene (in a combination with acetylene linker), 2-methylthiothiophene, methoxy or thiomethyl moiety were employed. All synthesized catalysts were fully spectrally characterized and their fundamental properties were further investigated by X-ray analysis, electrochemistry, electronic absorption and emission spectra. The experimental results were supported by theoretical DFT calculations. Structure vs. catalytic activity relationship have been elucidated in three photoredox reactions including cross-dehydrogenative coupling and annulation reactions.

Keywords

photoredox catalysis, push-pull chromophore, intramolecular charge-transfer, pyrazine

Abstrakt

Byla provedena literární rešerše v oblasti fotoredox katalýzy organickými substancemi, ze které vyplynulo šest skupin organických sloučenin nejčastěji využívaných ve fotoredox katalýze viditelným světlem. Byly shrnuty jejich základní fotofyzikální a elektrochemické vlastnosti a jejich využití v konkrétních fotoredox reakcích. V experimentální části byla provedena optimalizace přípravy již známého katalyzátoru. Dále byly provedeny strukturní modifikace tohoto katalyzátoru, které vedly k sedmnácti dalším sloučeninám s akceptorní části na bázi pyrazin-2,3-dikarbonitrilu, pyrazin-3,5-dikarbonitrilu, pyridin-2,6-dikarbonitrilu, pyridin-4-karbonitrilu a pyridin-3,5-dikarbonitrilu. Donorními částmi těchto sloučenin byl thiofen, 2-methoxythiofen a jeho kombinace s trojnou vazbou, 2-methylthiothiofen, methoxy nebo thiomethyl skupina. Všechny připravené sloučeniny byly plně spektrálně charakterizovány, jejich fundamentální vlastnosti byly dále studovány pomocí rentgenostrukturní analýzy, elektrochemických měření, absorpční a emisní spektroskopie, které byly podpořeny teoretickými DFT kalkulacemi. Vztahy mezi strukturou a katalytickými vlastnostmi byly dále studovány ve třech fotoredoxních reakcích, které zahrnují zkřížený dehydrogenativní kapling a anulační reakce.

Klíčová slova

fotoredox katalýza, push-pull chromofor, intramolekulární přenos náboje, pyrazin

Table of Contents

Acknowledgement

I would like to thank my supervisor prof. Filip Bureš for motivation, patience, and valuable advices. Further, I would like to thank my colleagues from the Department of Organic Materials Unit at the Institute of Organic Chemistry and Technology, Faculty of Chemical technology, University of Pardubice for friendly working environment. I especially thanks to Ing. Milan Klikar, Ph.D. for experimental support and electrochemical measurement, prof. Oldřich Pytela for DFT calculations and photoredox discussions and Martina Sebránková for kind attitude and flawless material support. My warmest thanks go to my boyfriend, who supported me even in the days of experimental failures and scientific crises. Finally, I would like to thank to my parents and Lany´s family, who encouraged me to start study and persistently supported me during my entire university studies.

1. Introduction

Over the last decade, photoredox catalysis became a unique tool for performing new chemical transformations. In general, term photoredox catalysis mean transformation of solar to chemical energy. Sunlight is natural and "unlimited" source of energy, which can be converted into chemical energy using a suitable photoredox catalyst. An essential demand for photoredox catalyst, no matter whether metal-based or organic, is the ability to undergo single electron transfer (SET) from/to excited catalyst to/from organic substrate. Photoredox reactions can be considered as an attractive alternative to the well-known organic protocols.[1,2] Well-studied classes of photocatalysts are transition metal complexes (eg. polypyridyl complexes of ruthenium and iridium) that have received a great attention and recognition, mainly for its versatility.[3] Another significant class of photoredox catalysis is dual catalysis, which mainly combines complexes of gold/iridium,[4] gold/ruthenium[5] and nickel/iridium.[6] All these metal complexes showed to be suitable photoredox catalysts with high catalytic activity. Modification of their structure is facile, but presence of expensive and toxic heavy metal is generally undesirable. Further, organic dyes (e.g. xanthene dyes such as fluorescein,[7] eosin Y,[8] eosin B[9] and rose Bengal[10]) represent attractive class of photoredox catalysts. Recently, synthesis of small organic molecules with photoredox properties become very burgeoning area. These compounds are easily available, cheap and feature great catalytic activity. Nevertheless, their further property tuning is very limited. Due to this reasons, attention turned to synthetic, organic substances that can be used as photoredox catalysts with tunable properties.[11] The current portfolio of synthetic organic photoredox catalysts consists mainly of cyanoarenes[12] as well as heteroaromatic substances such as flavins,[13] various pyridinium salts,[14] and perylene diimide.[15] The use of purely organic photocatalysts instead of transition metal complexes offers many advantages. The main advantages of organic photocatalysis include – lower cost compared to transition metal complexes, lower environmental impact, tunable photoredox properties, stability and solubility in organic solvents.[16] In general, an organic compound intended as photoredox catalyst should possess the following features:

- Absorption of the light within the UV/Vis region of the spectra.
- Absorption maxima should overlap the emission band of the light source.
- Ability to undergo photoinduced electron transfer or energy transfer.
- Easy regeneration of the catalyst.
- Sufficient solubility in the given reaction media.
- Inactivity towards substrate/product of the catalyzed reaction.
- Low catalyst loadings.

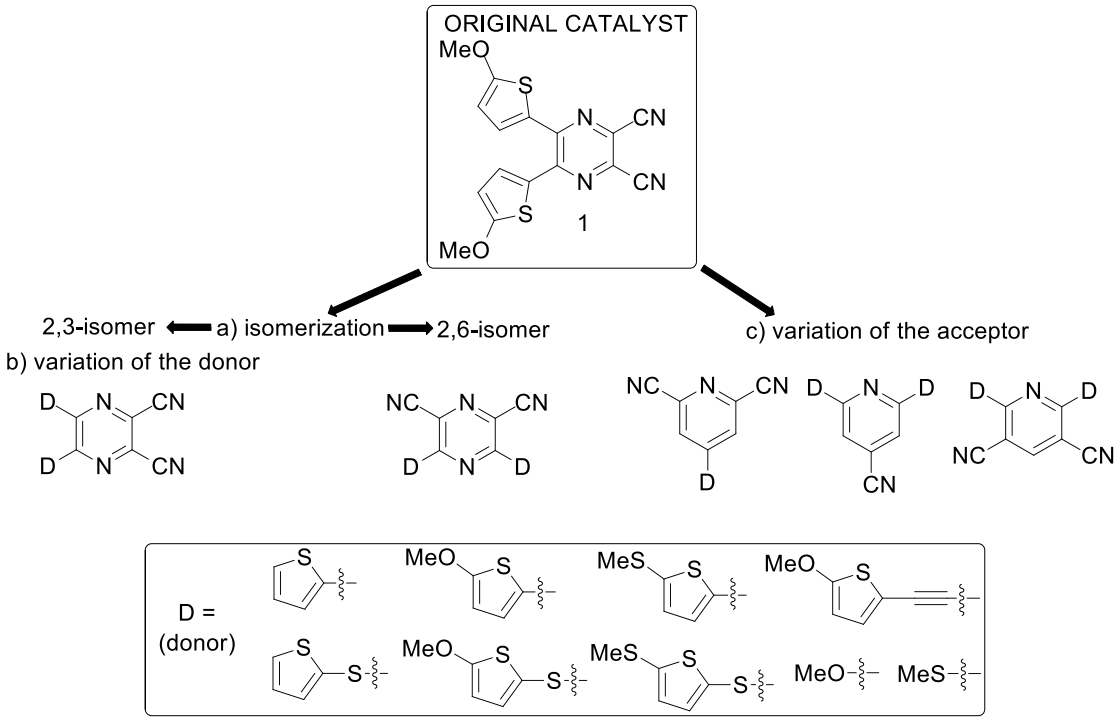

Figure 1. Structural modifications performed on original catalyst **1**.

This thesis reports herein an optimization of the synthesis of the known organic photocatalyst **1**. Its synthesis has already been published in 2014. While condensation method provided **1** in a very low yield (~ 3 %), the method using cross-coupling reaction ($Pd_2(dba)_3$/SPhos/Cs_2CO_3) provided **1** in high 86% yield.[16] New two-step one-pot reaction pathway leading to catalyst **1** has been developed. The synthesis is capable to afford high amounts of **1** and uses less expensive, less toxic, readily available, and stable starting materials. Subsequently, structural modifications of the original catalyst have been carried out leading to seventeen catalysts with acceptor part based on pyrazine-2,3-dicarbonitrile, pyrazine-3,5-dicarbonitrile, pyridine-2,6-dicarbonitrile, pyridine-4-carbonitrile and pyridine-3,5-dicarbonitrile (*Figure 1*). Various peripheral donors such as thiophene, 2-methoxythiophene (in a combination with acetylene linker), 2-methylthiothiophene, methoxy or thiomethyl moiety were employed. All synthesized catalysts were fully characterized and their fundamental properties were further investigated by X-ray analysis, electrochemistry and electronic absorption and emission spectra. The experimental results were further supported by theoretical DFT calculations. Structure vs. catalytic activity relationships have been elucidated in three photoredox reactions including cross-dehydrogenative coupling and annulation reactions.

2. Aims of thesis

- A literature search focused on synthesis and use of heterocyclic molecules in D-π-A arrangement and their possible applications in photoredox catalytic processes.
- Structural modifications of known catalyst based on pyrazine-2,3-dicarbonitrile and preparation of a systematic series of analogous catalysts.
- Structure and purity check for all target compounds.
- Testing catalytic activity of all target compounds in selected photoredox reactions.
- Interpretation of structure-properties-photoredox activity relationships.
- To develop, optimize, and industrially verify the new synthetic pathway leading to the known photoredox catalyst (5,6-bis(5-methoxythiophene-2-yl)pyrazine-2,3-dicarbonitrile).

3. Results and discussions

3.1. Synthesis

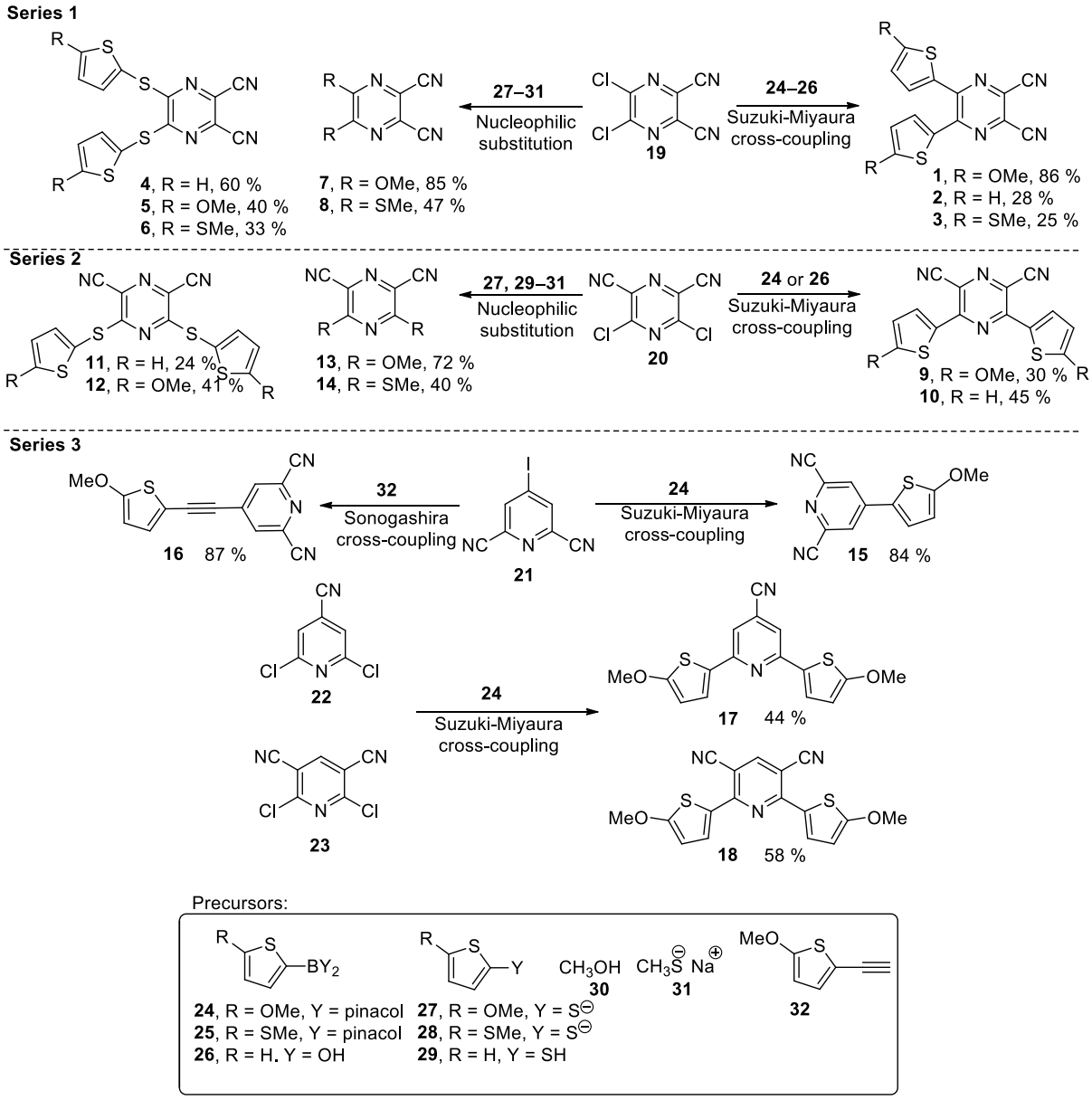

Scheme 1. Overall synthetic pathway leading to the target molecules **A1–18**.

Scheme 1 shows all synthesized catalysts, which can be divided into three series according to the selected acceptor unit: *series 1* (pyrazine-2,3-dicarbonitrile), *series 2* (pyrazine-2,6-dicarbonitrile) and *series 3* (pyridine-4-carbonitrile, pyridine-3,5-dicarbonitrile or pyridine-2,6-dicarbonitrile). Series 1 and 2 consist of X-shaped constitutional isomers. Series 3 provides molecules with both X- (**18**) and Y-shaped (**15–17**) arrangements. Target compounds **1–3**, **9–10** were synthesized via Suzuki-Miyaura reaction under optimized conditions (Cs_2CO_3, $Pd_2(dba)_3$, SPhos) in the yields of 25–86 %. The synthesis of target catalysts **4–8**, **11–14** was carried out by nucleophilic substitution. The syntheses of derivatives **7**, **8**, and **13** were reported previously.[17–19] Catalysts **15**, **17–18** were prepared by Suzuki-Miyaura cross-coupling under standard

conditions (Na_2CO_3, $PdCl_2(PPh_3)_2$) and were isolated in the yields ranging from 44 τo 87 %. Sonogashira reaction was used for the synthesis of **16**, extended by an acetylene liker. The synthetic strategy towards target molecules **1–18** utilizes commercially available 5,6-dichloropyrazine-2,3-dicarbonitrile **19**, its isomer 3,5-dichloropyrazine-2,6-dicarbonitrile **20** and pyridines **21–23**. Preparation of the acceptor unit **20** include five-step reaction sequence starting from malononitrile, its gradual nitrosation,[20] tosylation,[21] nucleophilic substitution with another molecule of malononitrile,[22] acid-catalysed cyclization[22] and final Sandmeyer reaction.[23] Pyridine **22** has been synthesized by a reaction of citric acid with urea,[24] and subsequent reaction of the resulting intermediate with phosphorus oxychloride.[25] Acceptor unit **23** was prepared in one-pot reaction of malononitrile with triethylorthoformate.[26] Precursors **26**, **29**–**31** as donor parts of the final catalysts were commercially available. Boronic acid pinacol esters **24** and **25** were synthesized by direct lithiation of thiophene moiety and subsequent reaction with *i*PrOBpin.[27,28] Thiolates **27** and **28** were generated *in-situ* from the corresponding thiophene derivative and its gradual lithiation and reaction with sulphur. The synthesis of terminal acetylene **32** started from 2-methoxythiophene, its iodination,[29] subsequent Sonogashira reaction with ethynyltrimethylsilane[29] and deprotection of TMS protecting group in the last step.[30]

The second main aim of my thesis was to develop a new and more suitable methodology for preparing known catalyst **1**. The published methods include condensation of dicarbonyl compound with diaminomaleonitrile, which led to the catalyst **1** in a very low 3% yield. The second known method consists of Suzuki-Miyaura cross-coupling under optimized conditions and provides **1** in 86% yield. Its significant drawbacks are use of expensive and relatively toxic heavy metal.[16] With the aim to commercialize catalyst **1**, a new reaction pathway leading to **1** was my goal. To avoid generic copying, four additional analogues of 2-methoxythiophene **33** have been synthesized according to *Scheme 2.* The reaction of 2-methoxythiophene **33** with appropriate alcohol in toluene catalysed by *p*-toluenesolfonic acid[31] afforded alcoholes **34–37** in 28–38% yields.

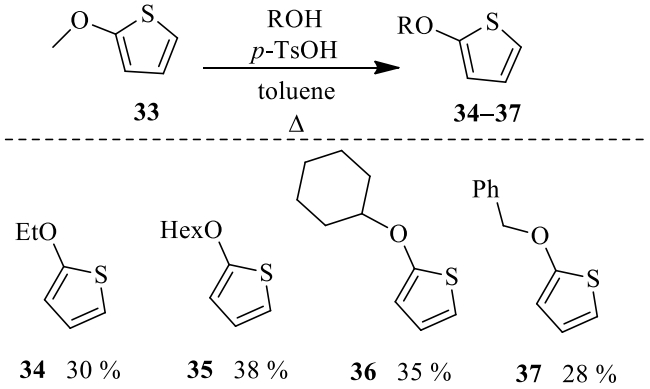

Scheme 2. Preparation of alkoxythiophenes **34–37**.

All prepared alcohols were utilized in the synthesis of known **1** and its four structural analogues **40**–**43** (*Scheme 3*). Screening of Lewis acids, solvents, reaction temperatures revealed $TiCl_4$/pyridine in 1,2-dichloroethane a suitable system for two-step one-pot synthesis of **1** and **40**–**43**. In addition, the entire synthesis has technologically been verified on a multigame scale in collaboration with COC company.

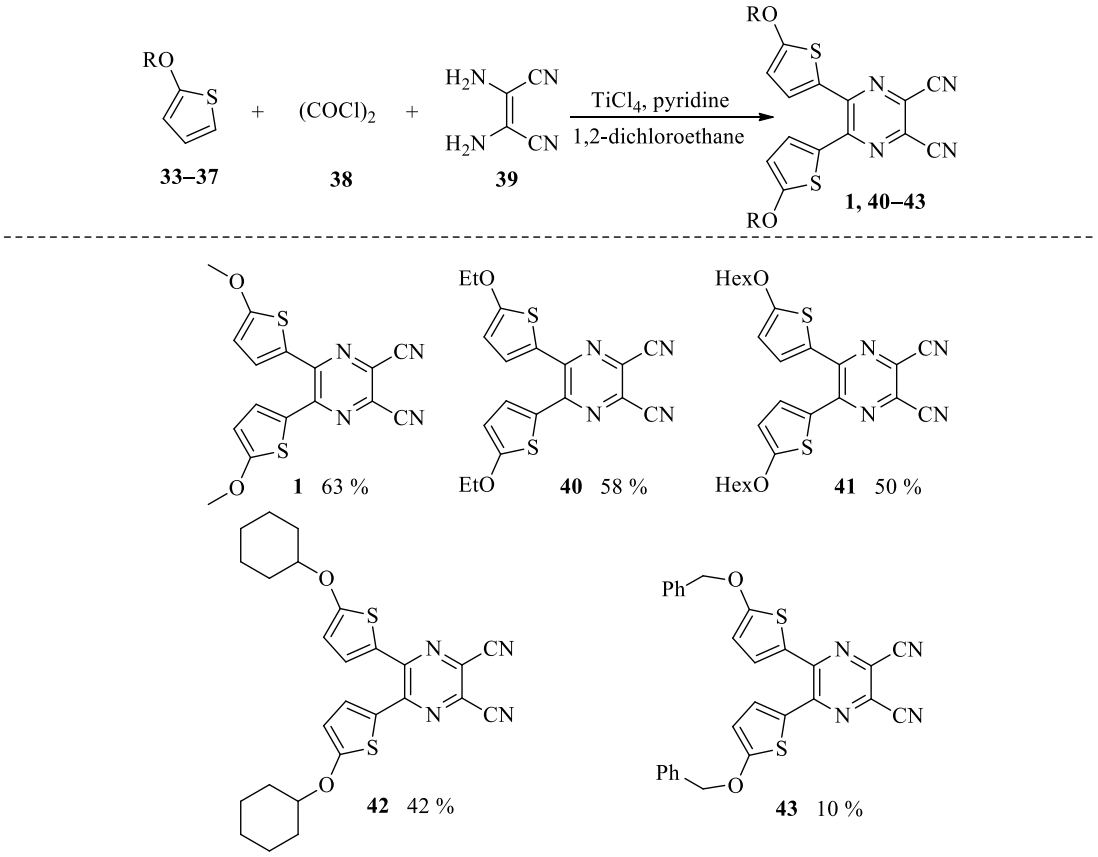

Scheme 3. One-pot synthesis leading to pyrazines **1**, **40–43**.

3.2. X-Ray analysis

Suitable single crystals of compounds **7** and **12** were prepared by a slow evaporation and hexane diffusion to their DCM solutions. X-ray analyses of parent compounds **1** and **2** have been published previously.[32] *Figure 2* shows ORTEP plots of all aforementioned derivatives. As can be seen from the dimethoxy derivative **7**, the parent DPZ adopts almost planar arrangement with the torsion angle below 1.5 ° (see the side view). However, both thiophene rings in **1** and **2** showed considerable twist with the torsion angle between 15-35 °. As a result, the dicyanopyrazine moiety in **1** and **2** is curved with the inner torsion angles between 5-15 °. In contrast to 2,3-isomers (**1**, **2** and **7**), 2,6-isomer **12** with sulfidic linker adopts completely different arrangement. Whereas the dicyanopyrazine acceptor is planar, both 5-methoxythiophenes appended at positions 3 and 5 are perpendicularly localized below the pyrazine ring. Orientation of both rings is reverse and parallel with mutual distance about 4 Å. D-A interaction in particular push-pull molecules has been estimated through aromaticity Bird index of the pyrazine and thiophene rings.[33–36] The pyrazine rings in **1**, **2**, **7** and **12** possess I_6 values of 81.8, 84.4, 71.2 and 90.8. A comparison to unsubstituted pyrazine (I_6 = 88.8) reveals higher bond length alternation and thus higher intramolecular charge transfer in 2,3-isomeric **1**, **2** and **7**. 2,6-Isomer **12** possesses higher aromaticity than pyrazine and, therefore, the extent of the intramolecular charge transfer is lower. This results from the additional sulfidic linker that i) is generally weaker electron donor than methoxy group (such as in **7**),[29] ii) separates 5-methoxythiophene moiety from the pyrazine acceptor and

disallows their mutual D-A interaction and iii) delocalizes its lone electron pairs also partially to the appended thiophene. Average Bird index of thiophene rings in **1**, **2** and **12** are 61.6, 64.3 and 59.8. Taking I_5 = 66 as a reference value for unsubstituted thiophene, thiophene rings in **12** seem to be the most polarized but these are not in a direct conjugation to DPZ acceptor. Methoxy groups appended at thiophene as in **1** cause also significant polarization as compared to unsubstituted derivative **2**.

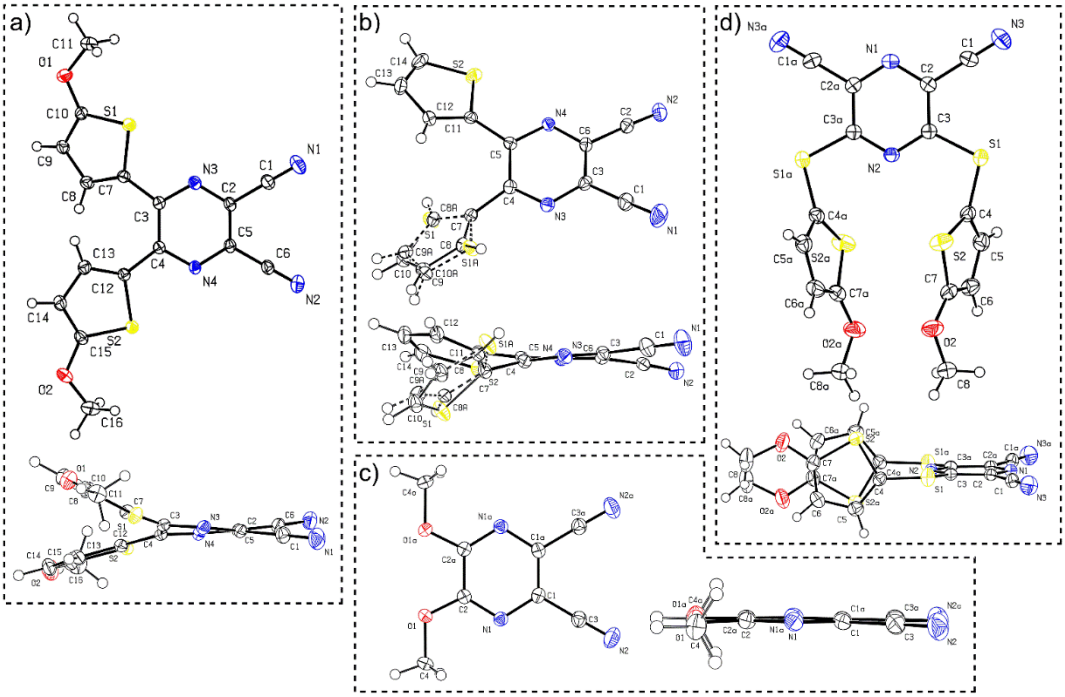

Figure 2. ORTEP representations of DPZ derivatives a) **1** (CCDC 1553203), b) **2** (CCDC 1553204), c) **7** (CCDC 1897538) and d) **12** (CCDC 1897539). Vibrational ellipsoids obtained at 150 K are shown at the 50% probability level, R = 0.04-0.05. Top and side views are provided.

3.3. Photophysical properties

The color of all prepared derivatives **1**–**18**, **40–43** ranges from yellow to red. Their fundamental photophysical properties were measured in dichloromethane (*Table 1*) and acetonitrile (*Table 2*) at concentration 2 × 10^{-5} M. The electronic absorption spectra of all derivatives are shown in *Figure 3* as a dependence of the molar extinction coefficient (ε) on the wavelength (λ). *Table 1* summarizes the measured longest-wavelength absorption maxima (λ_{max}^{A}) and corresponding molar extinction coefficients (ε). Absorption and emission properties, Stokes shift, quantum yield, DFT calculated value of absorption maxima and excited state energy $E_{0,0}$ of **1–18** in acetonitrile are shown in *Table 2*. The longest wavelength absorption maxima are located within the spectral range of 276 to 459 nm. *Figure 3* is divided into four parts according to the catalysts structure. In *Figure 3a* pyrazine derivatives **1–8** based on pyrazine-2,3-dicarbonitrile are shown; analogously *Figure 3b* displays electronic absorption spectra of **9–14** based on pyrazine-5,6-dicarbonitrile. Absorption spectra of pyridine derivatives **15–18** are shown in *Figure 3c*, whereas *Figure 3d* show spectra of catalysts **1**, **40–43**.

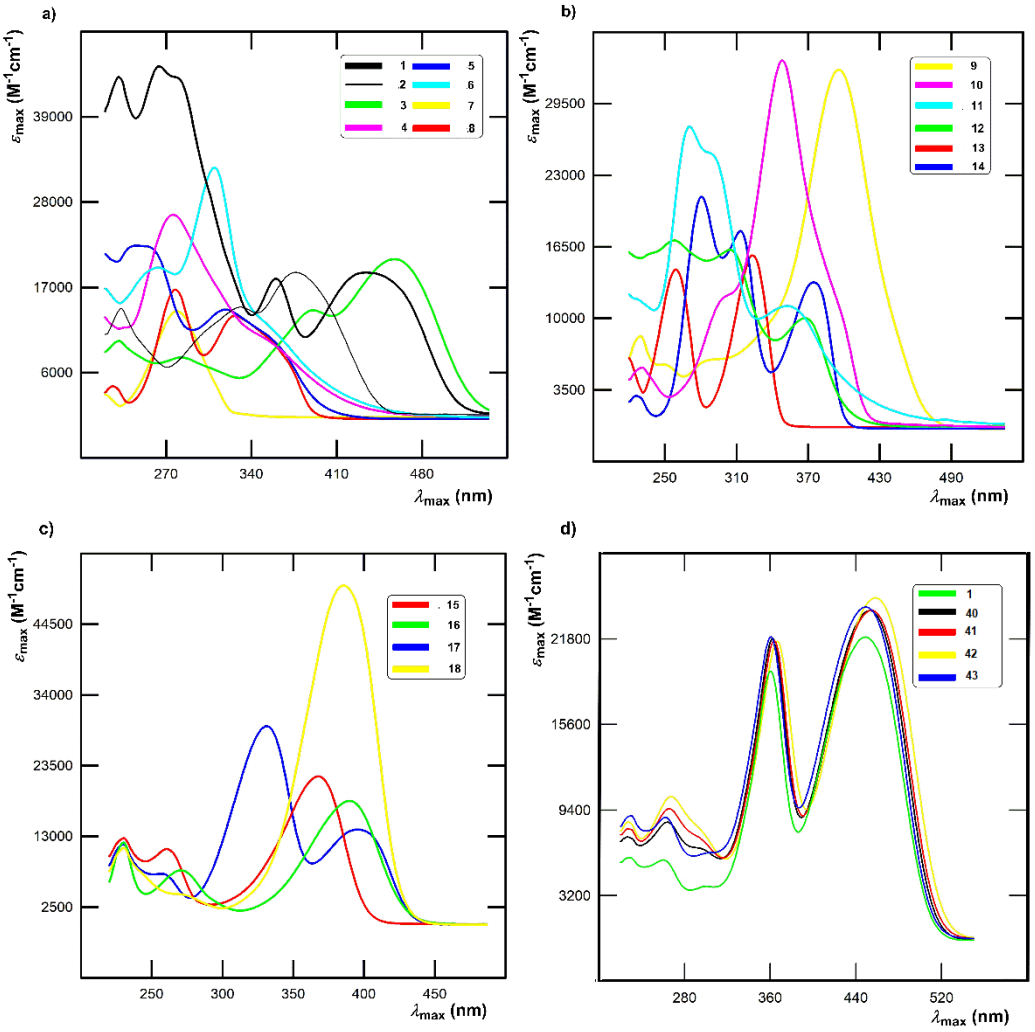

Figure 3. UV-Vis absorption spectra of synthesized derivatives measured in DCM.

Table 1. Photophysical properties of target compounds **1**–**18**, **40**–**43** measured in DCM.

Compound	λ_{max}^{A} [nm/eV]	ε [$M^{-1}cm^{-1}$]	Compound	λ_{max}^{A} [nm/eV]	ε [$M^{-1}cm^{-1}$]
1	450/2,76	19 000	**12**	369/3,36	10 100
2	389/3,19	19 000	**13**	324/3,83	16 400
3	459/2,70	20 700	**14**	376/3,29	13 400
4	276/4,49	26 600	**15**	369/3,36	22 100
5	320/3,88	14 200	**16**	391/3,17	18 400
6	310/4,00	33 000	**17**	397/3,12	14 100
7	278/4,46	14 200	**18**	385/3,22	50 600
8	326/3,80	13 500	**40**	454/2,73	23 900
9	396/3,13	32 800	**41**	456/2,72	24 000
10	349/3,55	34 000	**42**	458/2,71	24 900
11	357/3,47	11 100	**43**	450/2,76	24 200

Table 2. Photophysical properties of target compounds **1**–**18** measured in MeCN.

Comp	λ_{max}^{A} [nm/eV]	λ_{max}^{F} [nm/eV]	q^{F}	*Stokes shift* [cm^{-1}/eV]	$E_{0,0}$ [a] [eV]	λ_{maxDFT} [b] [nm/eV]
1	440/2,82	571/2,17	<0,02	5200/0,65	2,50	454/2,73
2	379/3,27	488/2,54	<0,02	5900/0,73	2,91	402/3,08
3	443/2,79	552/2,20[c]	<0,02[c]	4100/0,51[c]	2,22[c]	472/2,63
4	279/4,44	-	-	-	-	335/3,70
5	315/3,94	-	-	-	-	337/3,68
6	307/4,04	-	-	-	-	363/3,42
7	278/4,46	349/3,55	0,024	7300/0,91	4,00	279/4,44
8	323/3,84	409/3,03[c]	-	6300/0,78[c]	2,97[c]	340/3,65
9	389/3,19	562/2,21	<0,02	4500/0,98	2,70	420/2,95
10	343/3,62	462/2,68	<0,02	7600/0,93	3,15	380/3,26
11	351/3,53	-	-	-	-	342/3,63
12	363/3,42	-	-	-	-	345/3,60
13	322/3,85	363/3,42	0,18	3600/0,43	3,64	297/4,18
14	371/3,34	417/2,97	<0,02	3000/0,37	3,16	350/3,55
15	362/3,36	464/2,67	0,03	6000/0,75	3,02	343/3,62
16	378/3,17	-	-	-	-	381/3,25
17	391/3,12	485/2,56	0,06	5000/0,61	2,84	403/3,08
18	377/3,22	508/2,44	0,02	6800/0,85	2,83	392/3,16

[a] Excited state energy, calculated as the midpoint between absorption and emission maximum (Ref. [11]); [b] DFT calculated values in vacuum [c] Measured/calculated using emission maxima obtained in DCM.

The following conclusions can be drawn by comparing the spectral characteristics of all catalysts:

- Whereas spectrum of parent **1** contains two well-developed CT-bands, isomer **9** showed a single peak located between the two peaks of **1**. This observation distinguishes quadrupolar and linear nature of **1** and **9** (the pair **2** and **10** likewise).
- Effect of the peripheral donor is demonstrated on representative derivatives **9** and **10**, both with single narrow absorption peak. When going from **10** to **9**, thus attaching two methoxy groups, the longest-wavelength absorption maxima shifts bathochromically by almost 50 nm.
- Further replacement of OMe with SMe groups, as for instance in **13**/**14** or **7**/**8**, is accompanied by a similar red shift. The same trend has also been observed in well-developed series **2**/**1**/**3** (H/OMe/SMe).
- However, increasing donating ability of the R-substituents in subseries **4**–**6** or **11**–**12** has rather opposite effect, which reflects non-conjugate arrangement due to

a sulfidic bridge. Its impact can further be demonstrated by comparing representative chromophores **3** and **6**, both with SMe peripheral donors. The latter showed substantially blue shifted spectra by 136 nm.

- Truncation of the π-system has very similar effect e.g. for chromophores **1** and **7**. The CT-band of **7** is positioned hypsochromically by 162 nm in comparison to **1**.
- When going from pyrazine (catalyst **1**) to pyridine (catalyst **18**) central core of the catalyst, significant increase of the molar absorption coefficient is observed.
- Introduction of acetylene linker into the catalyst **15**, results in planarization of the molecule and 20 nm bathochromically shifted CT-band of catalyst **16**.

Absorption spectra of catalysts **40–43** (*Figure 3d*) showed almost identical behaviour as expected. They differ at least in both the absorption maxima and molar extinction coefficient. The largest difference (still minor) can be found when comparing molar extinction coefficients of catalyst **1** and **42**, equipped with cyclohexyl group. Thus, the various alkyl groups have a minor influence on the optical properties of **40**–**43**.

3.4. Electrochemistry

The electrochemical behavior of the target catalysts **1**–**18** was investigated by cyclic voltammetry (CV) in acetonitrile. All measured potentials are shown in *Table 3*. The half-wave potentials of the first oxidation ($E_{1/2(ox1)}$) for catalysts **1–6, 9, 11–12** and **15–18** are irreversible processes, values of oxidation potentials of catalysts with truncated π-system **7–8/13–14** and **10** with appended thiophene moiety without peripheral donor are located out of the MeCN potential window. The reductions ($E_{1/2(red1)}$) are irreversible (**4–7, 11–12, 14**), quasi- (**8**, **13**, **15–16**) or reversible (**1–3**, **9–10**, **17–18**) processes.

Table 3. Electrochemical properties of the final catalysts **1**–**18**.

Comp.	Ground state					Excited state	
	$E_{1/2(ox1)}$ [a] [V]	$E_{1/2(red1)}$ [a] [V]	ΔE [b] [V]	E^{el}(HOMO) [c] [eV]	E^{el}(LUMO) [c] [eV]	E^{*}_{ox} [d] [V]	E^{*}_{red} [d] [V]
1	1,32	–1,14	2,46	–5,79	–3,33	–1,18	1,36
2	1,75	–1,12	2,87	–6,22	–3,35	–1,16	1,79
3	1,32	–1,01	2,33	–5,79	–3,46	–0,90[e]	1,21[e]
4	1,31	–1,00	2,31	–5,78	–3,47	-	-
5	1,82	–0,97	2,79	–6,29	–3,50	-	-
6	1,25	–0,95	2,20	–5,72	–3,52	-	-
7	-	–1,53	-	-	–2,94	-	2,47
8	-	–1,23	-	-	–3,24	-	1,74[e]
9	1,57	–1,15	2,72	–6,04	–3,32	–1,13	1,55
10	-	–1,04	-	-	–3,43	-	2,11
11	1,34	–1,00	2,34	–5,81	–3,47	-	-
12	1,79	–0,97	2,76	–6,26	–3,50	-	-
13	-	–1,41	-	-	–3,06	-	2,23
14	-	–1,16	-	-	–3,31	-	2,01
15	1,52	–1,44	2,96	–5,99	–3,03	–1,50	1,58
16	1,40	–1,25	2,65	–5,87	–3,22	-	-
17	1,24	–1,73	2,97	–5,71	–2,74	–1,60	1,11
18	1,47	–1,40	2,87	–5,94	–3,07	–1,36	1,43

[a] $E_{1/2(ox1)}$ and $E_{1/2(red1)}$ are peak potentials of the first oxidation and reduction, respectively; all potentials are given vs. SSCE [b] $\Delta E = E_{1/2(ox1)} - E_{1/2(red1)}$ (electrochemical gap); [c] $-E^{el}$(HOMO/LUMO) = $E_{1/2(ox1/red1)}$ + 4,429 (in MeCN vs. SCE) + 0,036 (difference between SCE (0,241 vs. SHE) and SSCE (0,205 vs. SHE)); [d] Excited state redox potentials in acetonitrile calculated as follows: $E_{ox}^{*} = E_{1/2\ (ox1)} - E_{0,0}$ a $E_{red}^{*} = E_{1/2(red1)} + E_{0,0}$ (Ref.[11]); [e] Measured/calculated using emission maxima obtained in DCM.

Whereas the first reduction takes place at the heteroaromate moiety, the first oxidation most likely involves MeO/MeS-substituted thiophene moieties. Since the half-wave potentials are not available for all studied compounds, $E_{p(ox1)}$ and $E_{p(red1)}$ values were recalculated to the HOMO/LUMO energies. Based on the measured electrochemical data, the following conclusions can be made:

- When comparing electrochemical behavior of 2,3- and 2,6-isomers, e.g. **1** vs. **9**, the latter showed deepened HOMO, unaltered LUMO and thus larger HOMO-LUMO gap.
- Attachment and variation of electron donors (H→OMe/SMe) significantly alters the HOMO energy. For instance, well-developed series of DPZs **2**/**1**/**3** (H/OMe/SMe) showed gradually reduced electrochemical HOMO-LUMO gap of 2,87/2,46/2,33 eV, which also correspond to red-shifted absorption spectra

- An insertion of the sulfidic linker reduces the electrochemical HOMO-LUMO gap.
- A truncation of the π-system by removing thiophene linker is less electrochemically obvious as oxidations of chromophores **7**–**8** and **13**–**14** are out of the potential window.

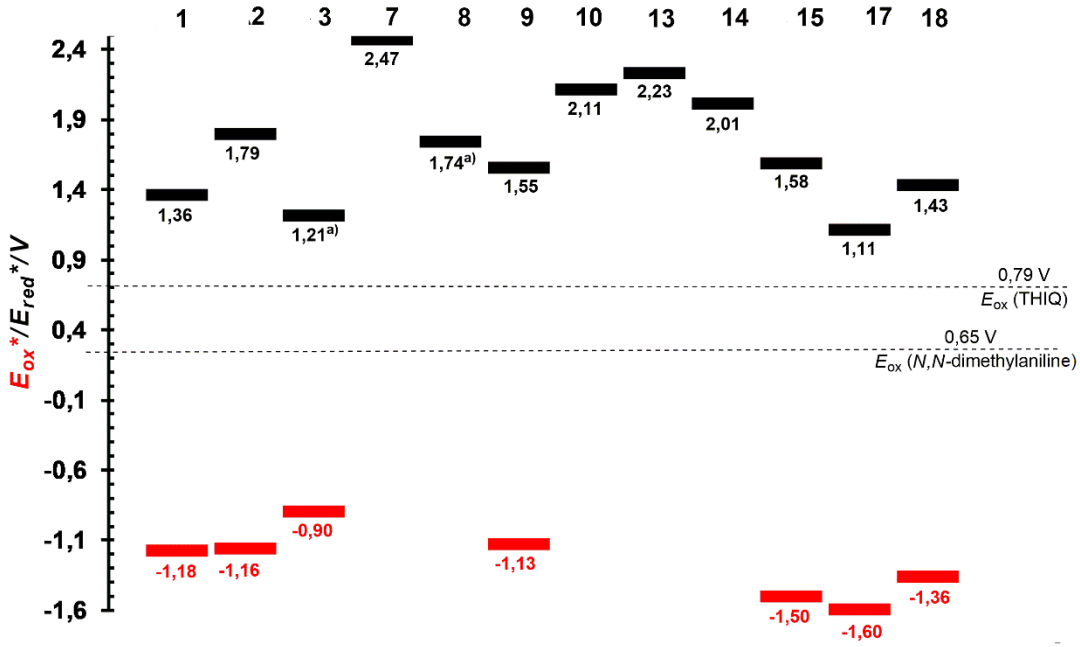

Figure 4. Excited state redox potentials.

The redox potentials of the excited states E_{ox}^* and E_{red}^* were calculated by combining the electrochemical peak potentials and the excited state energies $E_{0,0}$ (*Table 3*). Whereas the excited state oxidation potentials are almost unaltered, the principal changes are seen on the reduction potentials (*Figure 4*). Despite the limited data available, **1**–**18** seems to be strong oxidants with E_{red}^* up to 2,47 V.

3.5. DFT calculations

Quantum chemical calculations were run with DFT software package Gaussian, versions 09 (Ref.[41]) and 16 (Ref.[42]). Total energies of all possible conformers of derivatives **1**–**18** were calculated using the DFT B3LYP/6-311g(2d,p) method and, based on the lowest total energy, the most stable conformers were chosen. The DFT B3LYP/6-311++g(3df,2p) method involving symmetry constrains has been applied to optimize their ground state geometries as well as to calculate the corresponding radical cations, radical anions, dications, dianions and triplets in acetonitrile. The electronic absorption spectra, longest-wavelength absorption maxima λ_{max}^{DFT} (*Table 2*) and the corresponding electron transitions between molecular orbitals were calculated using TD-DFT method with B3LYP/6-311++g(3df,2p) basis set (nstates = 10).

Figure 5 shows frontier molecular orbital levels of the ground state (black) as well as spinorbitals of the species formed upon one electron transfer (blue, green and yellow). A comparison of the DFT and electrochemically obtained (red) HOMO/LUMO levels shows good agreement. *Figure 5* can be considered as fundamental for interpreting the photoredox catalytic properties of catalyst **1**.

Compared to non-ionized molecule, the radical cation possesses lower energy of the highest occupied orbital (αHOMO), which implies more difficult removal of an additional electron from the positively charged species. On the contrary, the αHOMO level of the radical anion is higher which facilitates abstraction of the electron from the negatively charged species. Physical interpretation can be carried out by ionization energy/potential of the electron in the orbital, which is given by a negative value of the energy of the particular orbital (Koopman's theorem).[43] Hence, ionization potential of the radical cation is higher, and radical anion lower, than that of non-ionized molecule. In triplet, the ground state HOMO is split into two spinorbitals α and β with higher and lower energy. The unpaired electron from the αHOMO can be transferred to another molecule to generate a radical cation. On the contrary, the partially occupied βHOMO may easily accept an electron from a molecule and form a radical anion. Both electron transfers from/to triplet are energetically very close to the levels of the radical cation/anion (*Figure 4*). The aforementioned mechanism is most likely responsible for visible light-induced photoredox activity of **1** and potentially also all other derivatives.
The CT-band of compounds **1**, **2** and **12** is solely generated by the HOMO→LUMO excitation. For remaining molecules, close orbitals such as HOMO-2/-1 and LUMO+1/+2 are also involved; a typically configuration interaction of two or exceptionally three (for **4** and **11**) electron transitions.

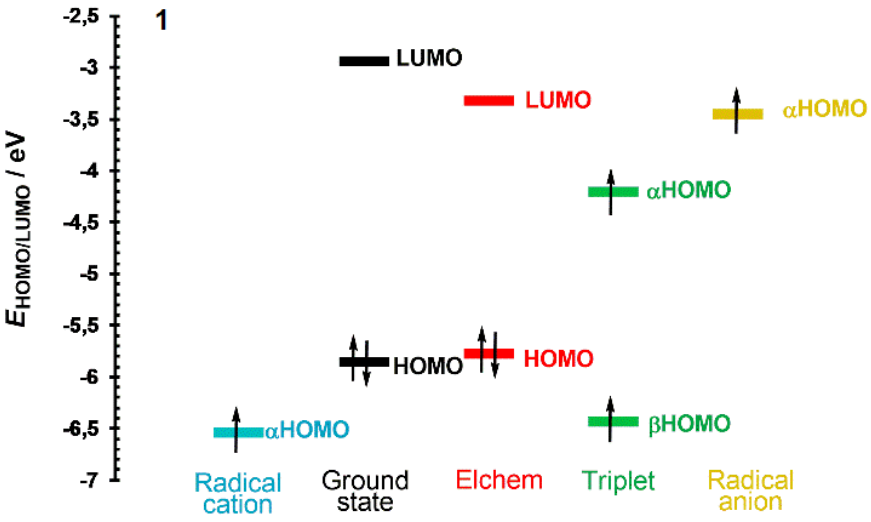

Figure 5. Energy level diagram of frontier molecular orbitals and spinorbitals of catalyst **1**.

3.6. Catalytic activity

The catalytic activities of all synthesized catalysts **1**–**18** (except catalyst **9**, due to its high instability) were firstly examined in benchmark cross-dehydrogenative coupling (CDC) reaction[37] between *N*-phenyltetrahydroisoquinoline (THIQ) **44** and nitromethane.

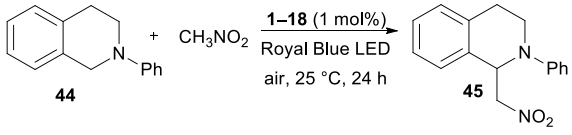

Scheme 4. Cross-dehydrogenative coupling.

In order to compare catalytic performance of all catalysts, the CDC reactions were carried out at standard conditions (1 mol% of the catalyst, Royal Blue LED source, 25 °C and 24 h reaction time). All reactions were repeated at least two times; the average isolated yields of **45** range from 75 to 96 %. All synthesized catalysts provided **45** in excellent yields (*Table 4*). Catalysts **1**, **6**, and **11** showed the best performance.

Table 4. Isolated yields of CDC reaction.

Catalyst	Isolated yield [%]	Catalyst	Isolated yield [%]
1	96	**10**	93
2	86	**11**	95
3	90	**12**	83
4	75	**13**	85
5	85	**14**	89
6	93	**15**	88
7	88	**16**	82
8	88	**17**	90
9	-	**18**	90

Secondly, the catalytic activity of **1**–**18** has further been screened in more challenging annulation reaction between *N*,*N*-dimethylaniline **46** and *N*-phenylmaleimide **47**. The first report on this reaction comes from Murata et al.[38] whereas its photoredox version has recently been reinvestigated.[39–47]

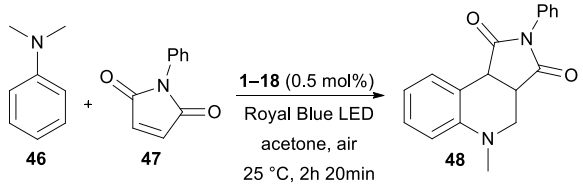

Scheme 5. Annulation reaction of **46** with **47**.

Catalytic activity of all prepared catalysts **1**–**18** (except **9**) have been verified in annulation reaction under optimized conditions. In contrast to CDC reaction, the catalytic performance of **1**–**18** in annulation reaction differs considerably. The best conversion and isolated yields of product **48** have been achieved with 2,3-isomers **1** (95 %) and **3** (94 %) with OMe and SMe donors. Both catalysts possess very similar optical and electrochemical properties, which led to their great and comparable catalytic activities.

Table 5. Isolated yields of annulation reaction.

Catalyst	Isolated yield [%]	Catalyst	Isolated yield [%]
1	95	**10**	36
2	73	**11**	13
3	94	**12**	32
4	14	**13**	11
5	7	**14**	7
6	7	**15**	11
7	14	**16**	15
8	10	**17**	21
9	-	**18**	14

Further, we turned our attention towards expanding the original maleimide to six-membered 1,2-dimethyl-1,2-dihydropyridazine-3,6-dione **49**. However, under the conditions optimized for annulation of *N*-phenylmaleimide **47**, no cyclization product has been observed. Whereas acetonitrile also proved to be unsuitable solvent, the reaction in 1,4-dioxane afforded an inseparable mixture of the desired product **50** and a noncyclic intermediate.

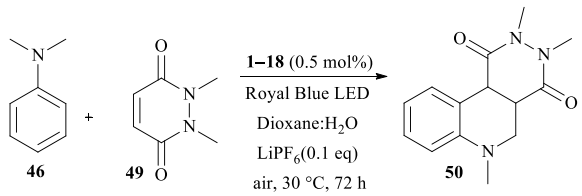

Scheme 6. Oxidative annulation of **46** and **49**.

Upon further solvent optimization and testing various Lewis acids ($ZnCl_2$, SmOTf, $LiPF_6$), we have successfully isolated the target pyridazino[4,5-*c*]quinoline derivative **50** in 40% yield. *Table 6* summarizes catalytic activity of all catalysts under optimized conditions and 72 h reaction time. Similarly, catalysts **1** and **3** proved to be most efficient and afforded **50** in the highest yields. Moreover, these two catalysts directed the reaction solely towards **50** with diminished side reactions such as oxidation and dimerization of the starting aniline **46**. Using **1** or **3**, the reaction can be completed within 10 days with the isolated yields of 93/90 %.

Table 6. Isolated yields of reaction *N*,*N*-dimethylaniline **46** and pyridazine **49**.

Catalyst	Isolated yield [%]	Catalyst	Isolated yield [%]
1	40/93[a)]	**10**	25
2	5	**11**	35
3	37/90[a)]	**12**	28
4	5	**13**	10
5	5	**14**	5
6	5	**15**	5
7	5	**16**	10
8	20	**17**	15
9	-	**18**	10

[a)] Reaction time 72/240 hours.

The structure-catalytic activity relationships can be generalized as follows:

- The lowest isolated yield (75 %) in a model CDC reaction was obtain with catalyst **4**. The reason may be its hypsochromically shifted CT band (λ_{MAX} = 279 nm) away from the light source (Royal Blue LED, ~430 nm). On the contrary, the highest isolated yield was achieved with known catalyst **1**. Its CT band overlaps the emission band of Royal Blue LED almost perfectly. All used catalysts enabled formation of product **45** in very high yields (83–95 %).
- In contrast to CDC reaction, much less catalysts were efficient in oxidative annulation between **46** and **47**. Known catalyst **1** and new **3**, which differ from **1** only in appended electron donor (OMe vs. SMe), showed great performance. Both catalysts possess very similar optical and electrochemical propertiesand afforded **48** in high 95 and 94% yields, respectively. Except suitable absorption properties, both derivatives possess narrow HOMO-LUMO gap and excited state reduction potentials (E^*_{red} = 1,36 resp. 1,21 V for **1** resp. **3**) close to the oxidation potential of *N*,*N*-dimethylaniline **46** (E_{ox} = 0,79 V). Catalyst **2** without appended peripheral donor provided satisfying 73% yield. All other catalysts enabled formation of **48** in relatively low 7–36% yields.
- Catalytic activity in annulation of **49** was significantly lower compared to two previous photoredox reactions. The best results were achieved with catalysts **1** and **3** (40 and 37 %). Surprisingly, catalyst **11** showed also good catalytic activity (35 %). Its HOMO-LUMO gap is almost comparable with **3** but value $E_{0,0}$ is not available. Lower activity could be due to its hypsochromically shifted absorption maxima (λ_{MAX} = 351 nm).
- When comparing 5,6- (**1–8**) and 3,5-disubstituted (**10–14**) dicyanopyrazines, 3,5-disubstituted derivatives showed significantly lower catalytic activity in the given photoredox reactions. The reason may be position of the absorption maxima, which is for catalysts **10–14** hypsochromically shifted. This results in less effective overlap with the emission band of the light source. The excited state reduction potentials E^*_{red} are higher for **10–14** than **1–8** and more are more far from E_{ox} of the substrates (**44**, **46**).

- Introduction of sulfidic linker to the catalyst structure (eg. **1** vs. **4**) results in hypsochromic shift of CT band ($\Delta\lambda_{MAX}$ = 161 nm) and significant decrease of the catalytic activity. Electrochemical properties stay almost unaltered.
- 2,5-Thienylene π-linker removal and direct connection of electron donors to the pyrazine ring e.g. catalyst **13**, results in undesirable hypsochromic shift of the absorption spectra (λ_{MAX} = 322 nm) from the LED source, increase of E^*_{red} (2,23 V) away from the oxidation potentials of used substrates and thus lower catalytic activity.
- Pyridine based catalysts **15**, **17** and **18**, in comparison to pyrazine **1**, are Y-shaped chromophores with decreased catalytic activity. Their absorption bands are slightly blue-shifted compared to **1**. This structural modification also led to the undesirable decrease of the reduction potentials and increase of the HOMO-LUMO gap.
- Introduction of the acetylene linker into the catalyst **15** led to the catalyst **16** with red-shifted CT-band by 16 nm. A difference in electrochemical properties of **15** and **16** is diminished, the HOMO-LUMO gap is slightly reduced. However, catalyst **16** was not able to properly catalyze annulation reaction and provide the desired product in the yields exceeding 15 %.
- Overall 5,6-disubstituted pyrazines without sulfidic linker with extensive conjugated system and peripheral OMe or SMe donors showed to be more suitable photoredox catalysts than 3,5-disubstituted pyrazines or (di)cyanopyridines.

4. Conclusion

In conclusion, I have performed structural modifications of known photoredox catalyst **1** and carried out a structure-catalytic activity study. Series of 18 compounds has been synthesized and could be divided into 3 series according to the structure. Series 1 consist of pyrazine-2,3-dicarbonitrile based compounds **1**–**8**, series 2 consist of six compounds based on pyrazine-2,6-dicarbonitrile **9**–**14** and four pyridine based compounds **15**–**18** form series 3. Target compounds have been synthesized using Suzuki-Miyaura/Sonogashira cross-coupling reactions or nucleophilic substitution. The target D-π-A molecules possess systematically altered structure with varied positions of the CN groups, different donors and linkers. The second aim of my work was to develop new reaction pathway towards known catalyst **1**. To avoid generic copying, four structural analogues of 2-methoxythiophene **33** have been prepared. Its synthesis started from reaction of **33** with appropriate alcohol catalyzed by *p*-toluenesulfonic acid. Alkoxyderivatives **33**–**37** have been used as a starting materials for the synthesis of **1** and its analogues **40**–4**3**. Screening of reaction conditions revealed $TiCl_4$/pyridine as a suitable catalytic system for two-step one-pot synthesis of **1** and **40**–**43**. In addition, the entire synthesis has technologically been verified on a multigame scale.

The X-ray analysis of all prepared catalysts **1**–**18** showed significant changes in spatial arrangements of target dicyanopyrazines depending on the substituents. The structural changes are also reflected in the optical and electrochemical properties of all catalysts. The optical and electrochemical gaps can be tuned within the wide range of 1,64 eV and 0,67 V, respectively; the excited state reduction/oxidation potentials were found up to 2,47/-1,60 V. The DFT calculations, especially diagram of frontier molecular orbitals and spinorbitals, allowed interpretation of photoredox fundamental properties of all catalysts. A tight correlation between the electrochemically measured and DFT calculated data with novel physico-chemical interpretation is provided. Finally, the photoredox activities of target catalysts have been examined in benchmark cross-dehydrogenative coupling as well as in novel annulation reactions. I have demonstrated superior photoredox activity of synthesized catalysts and first visible light induced formation of pyridazino[4,5-*c*]quinoline derivatives.

5. List of References

[1] D. A. Nicewicz, D. W. C. MacMillan, *Science* **2008**, *322*, 77–80.

[2] C. Stephenson, T. Yoon, *Acc. Chem. Res.* **2016**, *49*, 2059–2060.

[3] C. K. Prier, D. A. Rankic, D. W. C. MacMillan, *Chem. Rev.* **2013**, *113*, 5322–5363.

[4] Y. He, H. Wu, F. D. Toste, *Chem. Sci.* **2015**, *6*, 1194–1198.

[5] D. V. Patil, H. Yun, S. Shin, *Adv. Synth. Catal.* **2015**, *357*, 2622–2628.

[6] A. Noble, S. J. McCarver, D. W. C. Macmillan, *J. Am. Chem. Soc.* **2015**, *137*, 624–627.

[7] W. Guo, L. Q. Lu, Y. Wang, Y. N. Wang, J. R. Chen, W. J. Xiao, *Angew. Chem. Int. Ed.* **2015**, *54*, 2265–2269.

[8] M. Majek, A. J. Von Wangelin, *Angew. Chemie - Int. Ed.* **2015**, *54*, 2270–2274.

[9] M. Majek, F. Filace, A. J. Von Wangelin, *Chem. - A Eur. J.* **2015**, *21*, 4518–4522.

[10] H. Liu, W. Feng, C. W. Kee, Y. Zhao, D. Leow, Y. Pan, C.-H. Tan, *Green Chem.* **2010**, *12*, 953–956.

[11] N. A. Romero, D. A. Nicewicz, *Chem. Rev.* **2016**, *116*, 10075–10166.

[12] G. Pandey, S. Pal, R. Laha, *Angew. Chemie - Int. Ed.* **2013**, *52*, 5146–5149.

[13] V. Mojr, E. Svobodová, K. Straková, T. Neveselý, J. Chudoba, H. Dvořáková, R. Cibulka, *Chem. Commun.* **2015**, *51*, 12036–12039.

[14] N. J. Gesmundo, D. A. Nicewicz, *Beilstein J. Org. Chem.* **2014**, *10*, 1272–1281.

[15] M. Weiser, S. Hermann, A. Penner, H. A. Wagenknecht, *Beilstein J. Org. Chem.* **2015**, *11*, 568–575.

[16] Y. Zhao, C. Zhang, K. F. Chin, O. Pytela, G. Wei, H. Liu, F. Bureš, Z. Jiang, *RSC Adv.* **2014**, *4*, 30062–30067.

[17] E. H. Morkved, H. Ossletten, H. Kjosen, *Acta Chem. Scand.* **1999**, *53*, 1117–1121.

[18] T. Tetsuo, S. Hirozo, M. Takamaro, A. Toshiei, C. Michio, N. Akira, Patent: *2,3-Dicyanopyrazines*, **1981**.

[19] D. D. Scott, Patent: *Multifunctional pyrazines*, **1975**.

[20] M. F. Fathalla, S. N. Khattab, *J. Chem. Soc. Pakistan* **2011**, *33*, 324–332.

[21] G. Kinast, *European J. Org. Chem.* **1981**, 1561–1567.

[22] J. Perchais, J. P. Fleury, *Tetrahedron* **1974**, *30*, 999–1009.

[23] D. Vázquez Vilarelle, C. Peinador Veira, J. M. Quintela López, *Tetrahedron* **2004**, *60*, 275–283.

[24] S. W. J., T. H. Easterfield, *J. Chem. Soc. Trans.* **1893**, *63*, 1035–1051.

[25] J. Wibaut, J. P., Overhoff, *Recl. des Trav. Chim. des Pays-Bas* **1933**, *52*, 55–59.

[26] A. Duindam, V. L. Lishinsky, D. J. Sikkema, *Synth. Commun.* **2007**, *23*, 2605–2609.

[27] Z. Hloušková, F. Bureš, *Arkivoc* **2017**, *4*, 330–342.

[28] A. Cazzato, M. Zambianchi, M. Piacenza, F. Di Maria, G. Barbarella, F. Della Sala, G. Gigli, *J. Am. Chem. Soc.* **2009**, *131*, 10892–10900.

[29] B. Mühling, S. Theisinger, H. Meier, A. Oehlhof, E. Kirsten, *European J. Org. Chem.* **2006**, *2*, 405–413.

[30] I. Van Overmeire, S. A. Boldin, K. Venkataraman, R. Zisling, S. De Jonghe, S. Van Calenbergh, D. De Keukeleire, A. H. Futerman, P. Herdewijn, *J. Med. Chem.* **2000**, *43*, 4189–4199.

[31] N. Agarwal, C. H. Hung, M. Ravikanth, *Tetrahedron* **2004**, *60*, 10671–10680.

[32] F. Bures, J. Tydlitát, M. Kong, O. Pytela, T. Mikysek, M. Klikar, N. Almonasy, M. Dvořák, Z. Jiang, A. Růžička, et al., *Chem. Sel.* **2018**, 4262–4270.

[33] C. W. Bird, *Tetrahedron* **1986**, *42*, 89–92.

[34] C. W. Bird, *Tetrahedron* **1985**, *41*, 1409–1414.

[35] S. I. Kotelevskii, O. V. Prezhdo, *Tetrahedron* **2001**, *57*, 5715–5729.

[36] T. M. Krygowski, H. Szatylowicz, O. A. Stasyuk, J. Dominikowska, M. Palusiak, *Chem. Rev.* **2014**, *114*, 6383–6422.

[37] A. G. Condie, J. C. Gonzalez-Gomez, C. R. J. Stephenson, *J. Am. Chem. Soc.* **2010**, *132*, 1464–1465.

[38] S. Murata, K. Teramoto, M. Miura, M. Nomura, *Heterocycles* **1993**, *36*, 2147–2153.

[39] Z. J. Wang, S. Ghasimi, K. Landfester, K. A. I. Zhang, *Adv. Synth. Catal.* **2016**, *358*, 2576–2582.

[40] K. Sharma, B. Das, P. Gogoi, *New J. Chem.* **2018**, *42*, 18894–18905.

[41] M. Hosseini-Sarvari, M. Koohgard, S. Firoozi, A. Mohajeri, H. Tavakolian, *New J. Chem.* **2018**, *42*, 6880–6888.

[42] S. Firoozi, M. Hosseini-Sarvari, M. Koohgard, *Green Chem.* **2018**, *20*, 5540–5549.

[43] X. L. Yang, J. D. Guo, T. Lei, B. Chen, C. H. Tung, L. Z. Wu, *Org. Lett.* **2018**, *20*, 2916–2920.

[44] C. W. Hsu, H. Sundén, *Org. Lett.* **2018**, *20*, 2051–2054.

[45] J. T. Guo, D. C. Yang, Z. Guan, Y. H. He, *J. Org. Chem.* **2017**, *82*, 1888–1894.

[46] A. K. Yadav, L. D. S. Yadav, *Tetrahedron Lett.* **2017**, *58*, 552–555.

[47] A. K. Yadav, L. D. S. Yadav, *Tetrahedron Lett.* **2016**, *57*, 1489–1491.

6. List of Student´s Published Works

1. Filip Bureš, Zuzana Hloušková, Milan Klikar, Příprava a izolace 5,6-bis(5-methoxythiofen-2-yl)pyrazin-2,3-dikarbonitrilu v multigramovém měřítku, Centrum organické chemie, s.r.o; Rybitví, 30. 8. 2018, Verified Technology GAMA02/002/OT1.
2. License agreement between University of Pardubice and Santiago chemikálie s. r. o., subject – the use of applicant´s (University of Pardubice) invention entitled "Method of synthesis of 5,6-bis(5-alkoxythiophen-2-yl)pyrazine-2,3-dicarbonitriles, derivatives of dicyanopyrazine and use thereof", signed 25.2.2019.
3. Framework agreement between University of Pardubice and Santiago chemikálie s. r. o., subject - applicant´s (University of Pardubice) commitment to carry out the following work for the client (Santiago chemikálie s. r. o.) according to the individual subconcracts: 5,6-bis(5-methoxythiofen-2-yl)pyrazine-2,3-dikarbonitril, signed 21. 2. 2019.
4. Following application of the invention PCT/CZ2018/050014, European patent application (applied 6. 5. 2019) EP 18718091.4
5. Z. Hloušková, M. Klikar, O. Pytela, N. Almonasy, A. Růžička, V. Jandová, F. Bureš, *RSC Adv.* **2019**, *9*, 23797–23809.

Presented lectures

Zuzana Hloušková, Filip Bureš, Organic push-pull chromophores serving photoredox catalysis, Photochemistry Group Meeting, Telč, Czech Republic, **31.5–2.6.2019**

Presented posters

Zuzana Hloušková, Filip Bureš, Structural modifications of pyrazine-2,3-dicarbonitrile: Towards a series of efficient photoredox catalysts, Beilstein Organic Chemistry Symposium 2018, Potsdam, Germany, **24-26.4.2018**, pp.50

Zuzana Hloušková, Filip Bureš, Push-pull pyrazines in photoredox catalysis, Barrande-Vltava French-Czech Chemistry Meeting, Strasbourg, France, **27-28.8.2018**, pp. 81

Zuzana Hloušková, Filip Bureš, Pyridine push-pull derivatives as organic photocatalysts, 3rd International Caparica Conference on Chromogenic and Emissive Materials, Lisbon, Portugal, **3-6.9.2018**, pp. 196, ISBN 978-989-54009-6-6

Zuzana Hloušková, Filip Bureš, Pyrazine push-pull derivatives as photoredox catalysts, 24th RACI Organic Chemistry Conference ORGANIC18, Perth, Australia, **2-6.12.2018**

During my university studies, I published the following publications

Z. Hloušková, J. Tydlitát, M. Kong, O. Pytela, T. Mikysek, M. Klikar, N. Almonasy, M. Dvořák, Z. Jiang, A. Růžička, F. Bureš, *ChemistrySelect* **2018**, *3*, 4262–4270.

Z. Hloušková, F. Bureš, *Arkivoc* **2017**, *iv*, 330–342.